



Since January 2020 Elsevier has created a COVID-19 resource centre with free information in English and Mandarin on the novel coronavirus COVID-19. The COVID-19 resource centre is hosted on Elsevier Connect, the company's public news and information website.

Elsevier hereby grants permission to make all its COVID-19-related research that is available on the COVID-19 resource centre - including this research content - immediately available in PubMed Central and other publicly funded repositories, such as the WHO COVID database with rights for unrestricted research re-use and analyses in any form or by any means with acknowledgement of the original source. These permissions are granted for free by Elsevier for as long as the COVID-19 resource centre remains active.



# Structure-activity relationships of cryptopleurine analogs with E-ring modifications as anti-hepatitis C virus agents

Ying Wang<sup>a,b</sup>, Shao-Ru Chen<sup>b</sup>, Xiaoming Yang<sup>c</sup>, Kuo-Hsiung Lee<sup>c,d,\*</sup>, Yung-Chi Cheng<sup>a,\*</sup>

<sup>a</sup> Department of Pharmacology, Yale University School of Medicine, New Haven, CT 06520, United States

<sup>b</sup> Institute of Chinese Medical Sciences and State Key Laboratory of Quality Research in Chinese Medicine, University of Macau, Macau

<sup>c</sup> Natural Products Research Laboratories, Eshelman School of Pharmacy, University of North Carolina, Chapel Hill, NC 27599, United States

<sup>d</sup> Chinese Medicine Research and Development Center, China Medical University and Hospital, Taichung, Taiwan

## ARTICLE INFO

### Article history:

Received 24 October 2017

Revised 6 December 2017

Accepted 19 December 2017

Available online 20 December 2017

## ABSTRACT

The tylophorine analog *rac*-cryptopleurine exhibited potent anti-hepatitis C virus (HCV) activity through allosteric regulation of ATPase activity of heat shock cognate protein 70 (Hsc70). We evaluated the impact of modifications on the E-ring of *rac*-cryptopleurine to the inhibitory activity against HCV replication and regulation of ATPase activity of Hsc70. Cryptopleurine analog YXM-110 with a 13 $\alpha$ -hydroxyl group maintained activity against HCV and promoted ATP/ADP turnover of Hsc70; however, compounds with hydroxyl groups at other positions or with other orientations (YXM-109, YXM-139, and YXM-140) did not exhibit similar activities. Size modification or heteroatom incorporation of the E-ring led to loss of anti-HCV activity. Promotion of the chaperone activity of Hsc70 with carboxyl terminus Hsc70 interacting protein (CHIP) further enhanced the anti-HCV activity of *rac*-cryptopleurine and XYM-110. This structure-activity relationship (SAR) study refined structural design and optimization for developing *rac*-cryptopleurine analogs as potent anti-HCV agents targeted against the host factor involved in HCV replication.

© 2017 Elsevier Ltd. All rights reserved.

## 1. Introduction

Hepatitis C virus (HCV) infects >200 million people worldwide. Approximately 60%–80% of HCV infections progress into chronic diseases, including steatosis, cirrhosis, and liver cancer.<sup>1</sup> The standard of care for the treatment for HCV infection include pegylated interferon- $\alpha$  (IFN- $\alpha$ ), ribavirin, and IFN-free direct-acting antiviral (DAA) agents. The recent use of DAA, including protease inhibitors and polymerase inhibitors, have advanced the efficacy of anti-HCV agents to almost cure for most HCV genotypes.<sup>2</sup> However, DAA treatment is not suitable for patients with advanced infection that are with a high risk of liver failure, development of hepatocellular carcinoma, or death.<sup>2</sup> In addition, patients with a prior history of hepatocellular carcinoma and who have been treated with DAA for HCV infection have an unexpected high recurrence rate of liver cancer than previously predicted, with the recurrence rate of >40% in some subgroups.<sup>3</sup> In addition, the emerging resistance and high

cost of DAA treatment is still a high barrier that hinders broad access to patients.<sup>4</sup>

In addition to the HCV genome-encoded nonstructural (NS) proteins, host factors play essential functions in every step of the HCV life cycle. Drugs targeted at host factors, cellular components, or functions involved in viral life cycle are emerging as new therapeutic options for the management of HCV infection, especially potential agents to be used in combination with DAA.<sup>5</sup> For example, small molecule inhibitors that inhibit the peptidyl-prolyl *cis/trans* isomerase activity of cyclophilins can suppress replication of HCV, human immunodeficiency virus (HIV), and coronaviruses.<sup>5</sup> Our previous study suggested that heat shock cognate protein 70 (Hsc70) binds to the 3' untranslated region (NTR) and is involved actively in HCV replication.<sup>6</sup> Allosteric regulation of the ATPase activity of Hsc70 by tylophorine analogs DCB-3503 and *rac*-cryptopleurine perturbed translation of HCV RNA, which lead to inhibition of HCV replication.<sup>6</sup> *rac*-Cryptopleurine analogs exhibited inhibitory activities against several diseases, including cancer,<sup>7,8</sup> arthritis,<sup>9</sup> inflammation,<sup>10</sup> and dysentery.<sup>11</sup> We designed and synthesized a series of E-ring modified *rac*-cryptopleurine analogs,<sup>7,10</sup> which showed improved anti-cancer activity than the parent compounds.<sup>7,10</sup> We recently reported that tylophorine analog DCB-3503 perturbed translation of HCV RNA via disruption of the

\* Corresponding authors at: Department of Pharmacology, Yale University School of Medicine, New Haven, CT 06520, United States (Y.-C. Cheng); Natural Products Research Laboratories, Eshelman School of Pharmacy, University of North Carolina, Chapel Hill, NC 27599, United States (K.-H. Lee).

E-mail addresses: [khlee@unc.edu](mailto:khlee@unc.edu) (K.-H. Lee), [yccheng@yale.edu](mailto:yccheng@yale.edu) (Y.-C. Cheng).

replication complex, especially the binding between NS5A, NS5B, HCV RNA, and heat shock cognate protein 70 (Hsc70).<sup>6</sup> Despite the potency *rac*-cryptopleurine exhibited, the selection index of this compound to HCV replication and cytotoxicity is low ( $IC_{50}/EC_{50}$  is only <4 fold, Table 1). Modification of the E-ring of *rac*-cryptopleurine also changed the potency and inhibitory effect on NF- $\kappa$ B, AP-1, and CRE signaling pathways.<sup>12</sup> Therefore, modification on the E-ring has the potential to yield compounds with improved pharmacological profiles than *rac*-cryptopleurine. In this study, we determined the structural-activity relationship (SAR) correlations of E-ring modified *rac*-cryptopleurine analogs on anti-HCV activity and modulation of chaperone activity of Hsc70, aiming to provide insight into the structures that we could further modify to design new compound(s) having anti HCV activity with decreasing cytotoxicity.

## 2. Results and discussion

Previously, we established relationships between the anti-cancer activity and protein synthesis inhibitory effect of tylophorine and *rac*-cryptopleurine analogs with variously substituted and sized E-rings.<sup>12,13</sup> In this study, we focused on the effect of how E-ring modifications affect the anti-HCV activity. The modifications include addition of hydroxyl group with different configurations on the E-ring, enlargement of the E-ring, and heteroatom incorporation into the E-ring (Fig. 1). The anti-HCV activity was determined in Huh-luc/neo-ET cells harboring the HCV genotype 1b replicon. Among these analogs, compounds YXM-109, YXM-110, and YXM-140 maintained significant anti-HCV activity ( $EC_{50}$  1.4–4.9 nM) comparable or only slightly lower than that of *rac*-cryptopleurine ( $EC_{50}$  0.6 nM) (Table 1). However, the selectivity ratio of HCV activity ( $EC_{50}$ ) to cytotoxicity ( $IC_{50}$ ) increased for YXM-109 and YXM-140 (increased  $IC_{50}/EC_{50}$  ratio, Table 1). A change of the 12-hydroxyl moiety from a *beta*- (YXM-140) to an *alpha*-orientation (YXM-139) led to significantly decreased anti-HCV activity and cytotoxicity (Table 1). On the other hand, the same change with a 13-hydroxyl group increased anti-HCV activity and cytotoxicity (compare YXM-109 with YXM-110).

Incorporation of a secondary nitrogen atom at C-13 (YXM-66) or an oxygen atom at position-12 (YXM-82) in a six-membered E-ring caused significant loss of anti-HCV activity (Table 1). The presence of a tertiary nitrogen atom substituted with a dimethylamino group at position-12 (YXM-101) further decreased the anti-HCV activity (Table 1). Enlargement to a seven-membered

E-ring containing an additional carbon (YXM-83) or oxygen (YXM-142) decreased the anti-HCV activity compared with *rac*-cryptopleurine (Table 1). Compound YXM-93 with only a five-membered E-ring essentially lost anti-HCV activity (Table 1). In fact, any anti-HCV activity exhibited by YXM-82, YXM-93, and YXM-101 was primarily due to their cellular cytotoxicity, considering the marginal difference between their  $EC_{50}$  and  $IC_{50}$  values (low ratio of  $IC_{50}/EC_{50}$ , Table 1).

Hsc70 is actively involved in the replication of both HCV<sup>6,14</sup> and hepatitis B virus (HBV).<sup>15</sup> The C-terminal substrate binding domain of Hsc70 is an essential sequence for replication of both wide-type and lamivudine-resistant HBV,<sup>15,16</sup> and reduced replication of HBV DNA results from a decreased expression level of Hsc70, such as caused by RNA interference<sup>17</sup> or treatment with natural product oxymatrine,<sup>15</sup> its analogs,<sup>18</sup> or *N*-substituted matricin acid derivatives.<sup>19</sup> However, the cellular machinery required for replication of HBV, a partial double strand DNA virus, is distinct from that of HCV.<sup>20</sup> Treatment with *rac*-cryptopleurine or YXM-110 did not affect the expression level of Hsc70 for up to 72 h (Fig. 2A). We next assessed the anti-HBV activity of cryptopleurine analogs in HBV genome-integrated HepG2.2.15 cells (Table 1). The compounds'  $EC_{10}$  values against HBV were higher than their  $EC_{50}$  values against HCV (Table 1), suggesting that cryptopleurine analogs specifically inhibit HCV replication.

Host chaperone proteins and their client proteins are actively involved in viral life cycle. Cyclophilin A (CypA) directly regulated HIV infectivity by interacting with the *N*-terminal domain of HIV-1 capsid protein.<sup>21</sup> CypA also mediated HCV RNA binding to HCV NS5A and stimulated replication of HCV RNA.<sup>22</sup> Hsc70 co-localized with HCV particles in lipid droplet in the infected cells.<sup>14</sup> Hsc70 is also a major chaperone protein participating in the assembly of several subcellular complexes, for example HCV replication complex<sup>6</sup> and RNA-induced silencing complex.<sup>23</sup> The chaperone function of Hsc70 is governed by the *N*-terminal nucleotide binding domain (NBD) with ATPase activity.<sup>24</sup> Mutation of the ATPase pocket abolished the chaperone activity of Hsc70 and its binding to RNA.<sup>25,26</sup> By promoting the ATPase activity of Hsc70, *rac*-cryptopleurine and DCB-3503 inhibited HCV.<sup>6,26</sup> Thus, we next determined the impact of cryptopleurine analogs on the ATP/ADP turnover of Hsc70. Addition of *rac*-cryptopleurine enhanced ADP production by promoting the ATPase activity of Hsc70 at 10  $\mu$ M (Fig. 2B). The effect on Hsc70 ATPase activity of all cryptopleurine analogs were examined at 10  $\mu$ M in the same fashion as *rac*-cryptopleurine; only YXM-110 exhibited similar allosteric regulation of Hsc70 (Fig. 2).

**Table 1**

Activity of cryptopleurine analogs on HCV and HBV replication, and cytotoxicity to Huh-luc/neo-ET and HepG2.2.15 cells. Results shown are calculated from three independent experiments and depicted as mean  $\pm$  SD. Chemical structures are shown in Fig. 1.

	HCV (Huh-luc/neo-ET, 72 h)	HBV (HepG2.2.15, 6 d)			
	$EC_{50}$ (nM) <sup>a</sup>	$IC_{50}$ (nM) <sup>b</sup>	$IC_{50}/EC_{50}$	$EC_{10}$ (nM) <sup>c</sup>	$IC_{50}$ (nM)
<i>rac</i> -cryptopleurine	0.6 $\pm$ 0.1	2.0 $\pm$ 0.1 <sup>6</sup>	3.33	>30	6.3 $\pm$ 1.2
DCB-3503	31.5 $\pm$ 7.0	91.0 $\pm$ 11.0 <sup>6</sup>	2.89	>300	98.9 $\pm$ 7.2
YXM-109	4.9 $\pm$ 4.7	42.1 $\pm$ 1.2	8.59	>26	134.0 $\pm$ 28.0
YXM-110	1.4 $\pm$ 0.2	5.0 $\pm$ 4.1	3.57	>5.5	49.0 $\pm$ 15.0
YXM-139	246.1 $\pm$ 92.2	3.75 $\mu$ M	15.24	>3 $\mu$ M	1.6 $\pm$ 0.2 $\mu$ M
YXM-140	3.0 $\pm$ 1.6	21.3 $\pm$ 8.8	7.10	>25	258.0 $\pm$ 70.0
YXM-66	183.4 $\pm$ 61.1	1 $\mu$ M	5.46	>500	1.4 $\pm$ 0.2 $\mu$ M
YXM-82	650.6 $\pm$ 46.4	1 $\mu$ M	1.54	>500	1.1 $\pm$ 0.2 $\mu$ M
YXM-83	52.3 $\pm$ 7.1	0.5 $\pm$ 18.5	5.75	>1 $\mu$ M	2.7 $\pm$ 0.2 $\mu$ M
YXM-93	750.2 $\pm$ 34.8	1 $\mu$ M	1.33	>300	0.82 $\pm$ 0.13 $\mu$ M
YXM-142	16.7 $\pm$ 3.8	120.1 $\pm$ 17.0	7.19	>300	4.0 $\pm$ 0.2 $\mu$ M
YXM-101	3.75 $\mu$ M	4 $\mu$ M	1.07	>900	2.4 $\pm$ 0.4 $\mu$ M

<sup>a</sup>  $EC_{50}$ , the concentration of compound that inhibit 50% of HCV replication relative to vehicle (DMSO) treatment.

<sup>b</sup>  $IC_{50}$ , the concentration of compound that inhibit 50% of cell growth relative to vehicle (DMSO) treatment.

<sup>c</sup>  $EC_{10}$ , the concentration of compound that inhibit 10% of HBV replication relative to vehicle (DMSO) treatment.

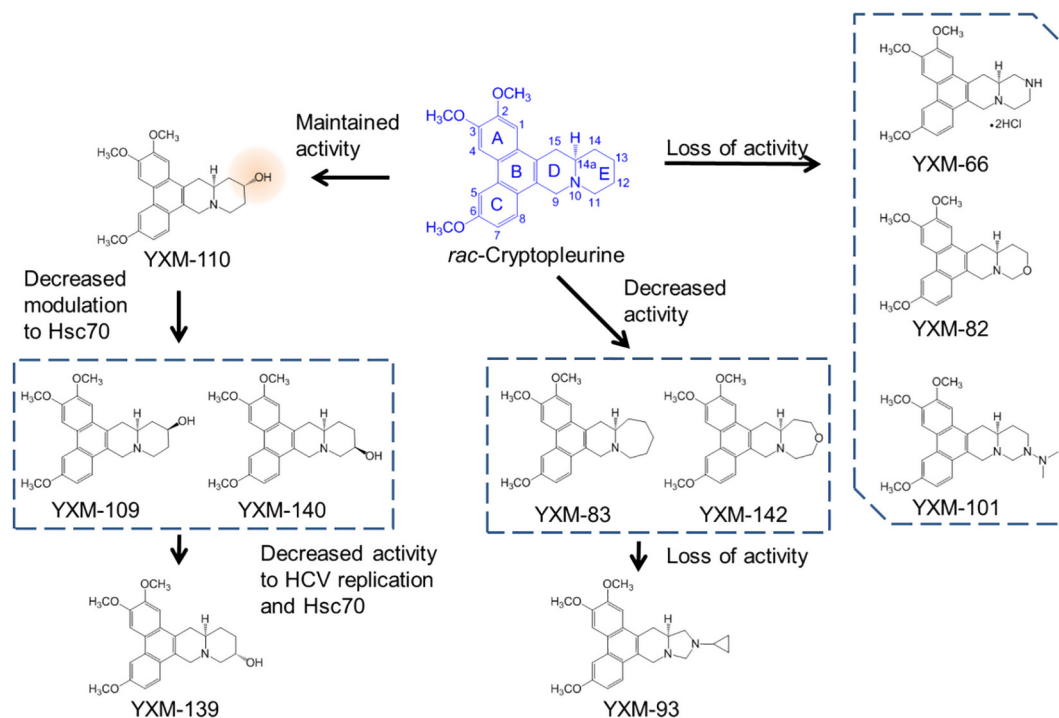


Fig. 1. Schematic description of the SAR of cryptoleurine analogs with E-ring modifications on anti-HCV activity.

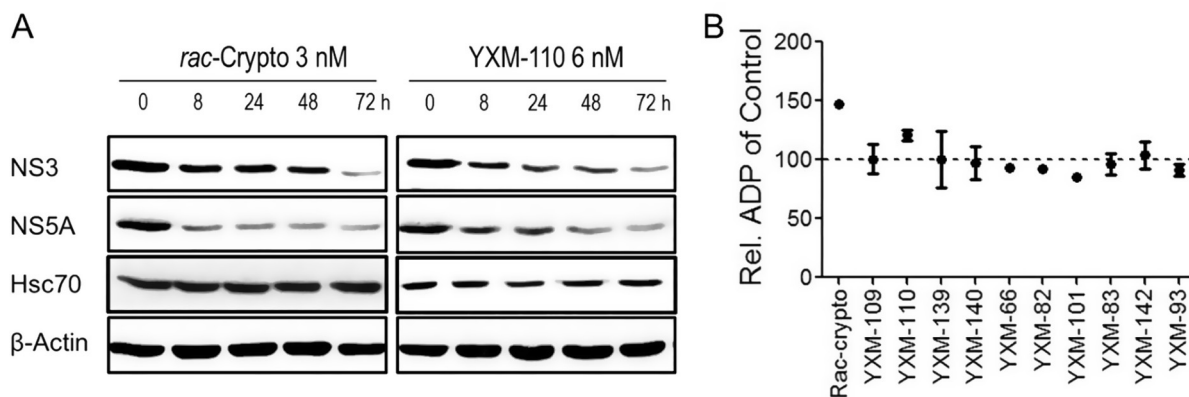


Fig. 2. The effect of cryptoleurine analogs on ATPase activity of Hsc70. (A) The expression level of NS3, NS5A, and Hsc70 under treatment with *rac*-cryptoleurine and YXM-110 in different time were analyzed by Western blot. (B) Ten micromole of each cryptoleurine analogs were added in the Hsc70 ATPase activity assay. The concentration of ADP produced was analyzed and calculated based on the area under the curve according to the standard curve generated on the same column. Results are resented as mean  $\pm$  SD from three separate experiments.

We previously that *rac*-cryptoleurine bound physically but non-covalently to the NBD of Hsc70<sup>6,26</sup>; therefore, functional analog(s) could interfere with the binding between *rac*-cryptoleurine and Hsc70. We next performed an affinity binding assay using biotinylated-*rac*-cryptoleurine,<sup>6,26</sup> and eluted Hsc70 bound to the affinity resin with *rac*-cryptoleurine or its analogs. YXM-110, but not YXM-109, YXM-139, nor YXM-140, eluted Hsc70 bound to the affinity resin in the similar fashion as that of *rac*-cryptoleurine (Fig. 3). This result together with the result in the ATP/ADP turnover assay suggested that YXM-110, but not other cryptoleurine derivatives, is a functional analog of *rac*-cryptoleurine with similar mechanism(s) of action. YXM-109 and YXM-140 may exhibited anti-HCV activity through other mechanism(s) rather than modulating ATPase activity of Hsc70. Analogs such as YXM-66, YXM-82, YXM-101, YXM-83, YXM-142, and YXM-93 lost the ability to modulate ATPase activity of Hsc70 (Fig. 3).

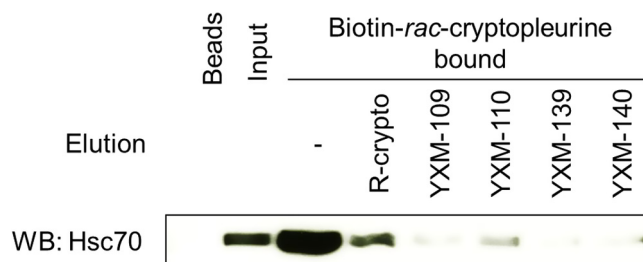
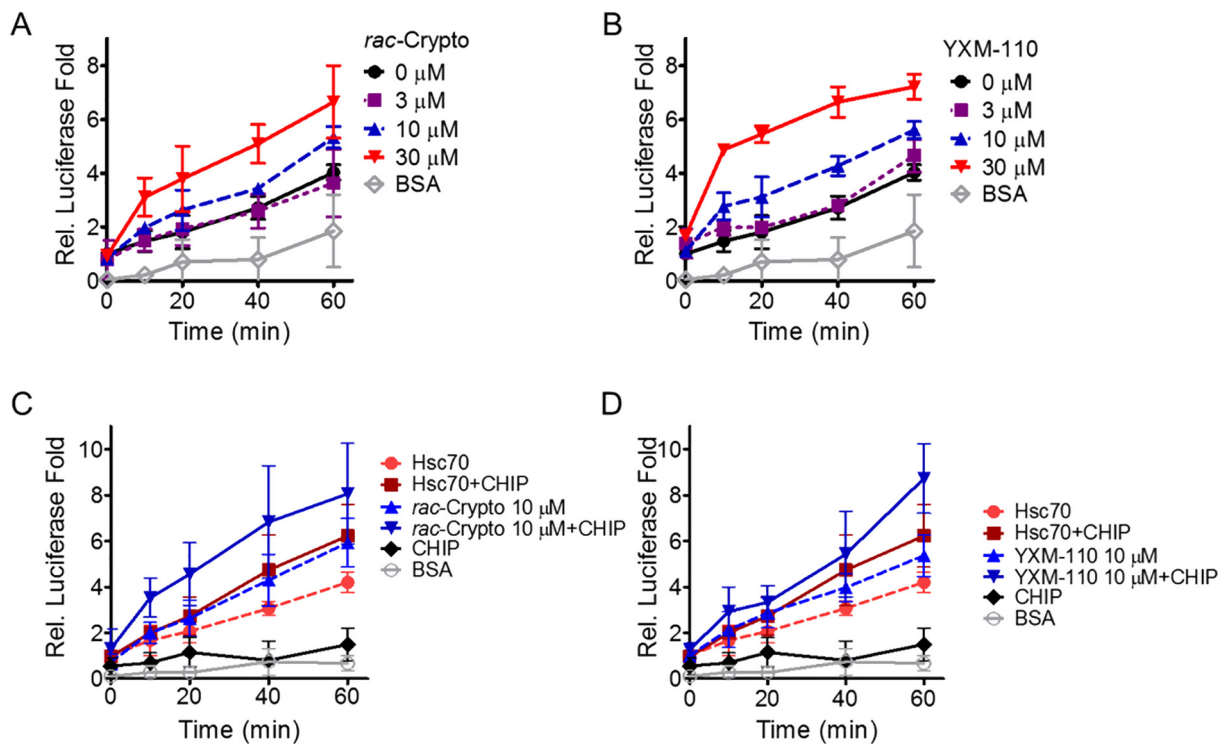
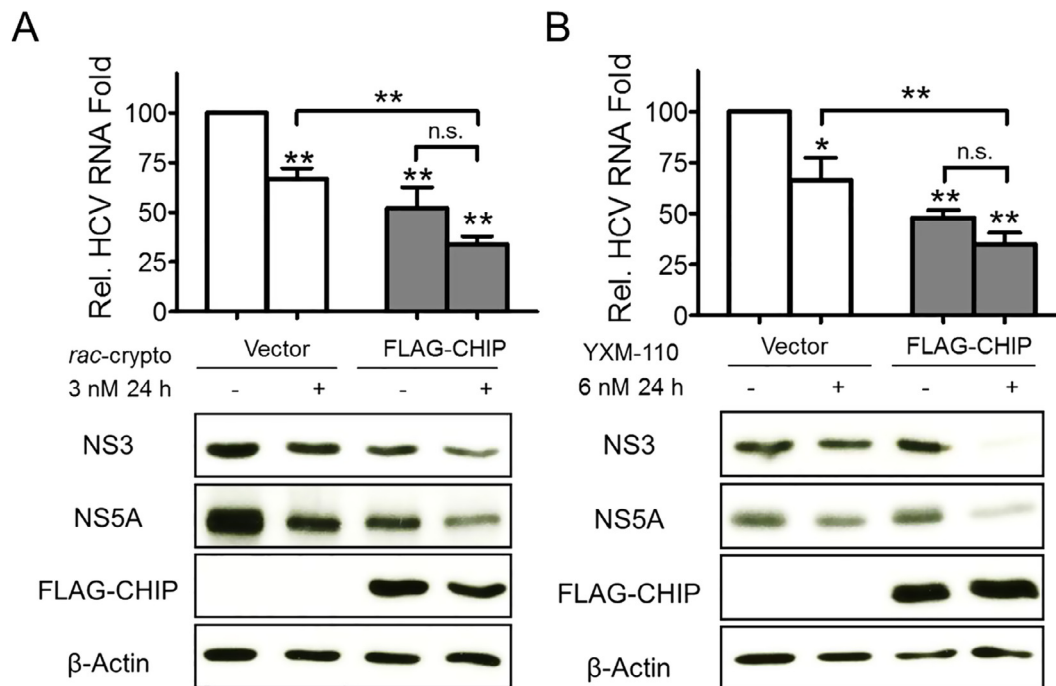


Fig. 3. YXM-110 dissociated binding between biotinylated-*rac*-cryptoleurine and Hsc70. Recombinant Hsc70 was incubated with biotinylated-*rac*-cryptoleurine resin for 2 h at room temperature. Hsc70 bound to the affinity resin were eluted with binding buffer alone or with *rac*-cryptoleurine, YXM-109, YXM-110, YXM-139, YXM-140, respectively. Hsc70 in each sample was resolved by Western blot analysis. Results are representative of two independent experiments.



**Fig. 4.** Characterization of effect of cryptopleurine analogs and cochaperone proteins on Hsc70 refolding activity. Relative reactivation of guanidine-denatured luciferase in the presence of difference dosages of (A) *rac*-cryptopleurine, and (B) YXM-110. Relative reactivation of guanidine-denatured luciferase with (C) *rac*-cryptopleurine, and (D) YXM-110 in the presence or absence of recombinant human CHIP. The results are presented as mean ± SD from three independent experiment.



**Fig. 5.** Regulation of Hsc70 cochaperone level enhanced anti-HCV activity of *rac*-cryptopleurine and YXM-110. The level of HCV RNA, NS3 and NS5A protein with the treatment of (A) *rac*-cryptopleurine or (B) YXM-110 for 24 h with transient transfection of FLAG-CHIP or empty vector (EV). The results are representative of more than two independent experiments (\*\*  $p < .01$ ; \*  $p < .05$ ; n.s., nonspecific).

The turnover of ATP/ADP of Hsc70 is primarily governed by its chaperone activity.<sup>27</sup> Co-chaperone protein nucleotide exchange factor c-terminal of Bag1 (cBag, or Bag-1 M) increased the ATPase

activity of Hsc70 in combination with *rac*-cryptopleurine or DCB-3503.<sup>26</sup> We then determined whether *rac*-cryptopleurine and YXM-110 affected luciferase refolding activity of Hsc70. Purified

native luciferase was first denatured with 6 M guanidine-HCl and incubated with Hsc70 in the presence or absence of *rac*-cryptopleurine or YXM-110. Luciferase activity was determined using 2  $\mu$ l aliquot of the reaction mixture at specific time point (Fig. 4). The luciferase reactivity was increased in both time- and dose-dependent manner with the addition of 10  $\mu$ M or higher concentrations of *rac*-cryptopleurine (Fig. 4A) and YXM-110 (Fig. 4B), indicating that these compounds enhanced chaperone activity of Hsc70. The carboxyl terminus Hsc70 interacting protein (CHIP) can enhance the protein refolding activity of Hsc70, thus promote ATP hydrolysis.<sup>27</sup> By promoting the degradation of heat shock protein 70 (Hsp70)-viral coat protein complex in potato virus<sup>28</sup> and Hsp90-viral polymerase complex in mumps virus,<sup>29</sup> CHIP regulated formation of viral replication complex and viral replication.

Accordingly, we added recombinant CHIP protein into the luciferase refolding reaction system. Recombinant CHIP by itself did not promote luciferase folding (Fig. 4C and D), and addition of CHIP alone only marginally promoted luciferase refolding activity of Hsc70 (Fig. 4C and D). However, the combination of CHIP and *rac*-cryptopleurine or YXM-110 further promoted the luciferase refolding activity of Hsc70 (Fig. 4C and D).

We next determined whether enhanced Hsc70 chaperone activity was related to the anti-HCV activity of cryptopleurine analogs. We transiently transfected FLAG-tagged CHIP plasmid or empty vector (EV) to Huh-luc/neo-ET cells with cryptopleurine analog treatment. Expression levels of HCV RNA, NS3 and NS5A proteins were downregulated by *rac*-cryptopleurine (Fig. 5A) or YXM-110 treatment alone (Fig. 5B). Overexpression of CHIP further enhanced the inhibition of HCV RNA, NS3 and NS5A protein levels, while the expression level of FLAG-CHIP was not changed (Fig. 5A and B). These results suggested that stoichiometric regulation of Hsc70 by cryptopleurine analogs was related to their anti-HCV activity.

In studies by Lai et al., YXM-110 exhibited anti-tumor activity in HCT116 xenograft model through abrogation of autophagy inhibitor 3-methyladenine and silencing of ATG5,<sup>8</sup> as well as inhibited protein synthesis through proteasome-dependent degradation of 4E-BP1.<sup>8</sup> We previously reported that *rac*-cryptopleurine and YXM-110 inhibited global protein synthesis.<sup>12</sup> Taken together, these results suggest that YXM-110 is a functional analog of *rac*-cryptopleurine, and could be used as a scaffold for future design of cryptopleurine analogs with higher potency against HCV and increased selectivity.

### 3. Conclusion

We evaluated the inhibitory activity of cryptopleurine analogs with E-ring modifications against HCV replication. Cryptopleurine analogs with different hydroxyl groups (YXM-110, YXM-109, YXM-140) exhibited improved selectivity between anti-HCV activities to cytotoxicity. Analogs with heteroatom modification of the E-ring (YXM-66, YXM-82, and YXM-101) exhibited cytotoxicity, but lost anti-HCV activity. The selectivity of YXM-139 increased compared with *rac*-cryptopleurine; however, the effects against HCV replication and Hsc70 ATPase promotion were diminished. Changing the size of the E-ring (YXM-142, YXM-93) or heteroatom modification (YXM-82) led to total loss of activity. Among all cryptopleurine analogs, YXM-110 exhibited similar anti-HCV activity and allosteric regulation of the ATPase activity of Hsc70 as *rac*-cryptopleurine as well as selectivity against HCV but not HBV (Fig. 1). Therefore, in addition to *rac*-cryptopleurine, YXM-110 could potentially be used alone or in combination with other anti-HCV regimens to high-barrier-to-resistance HCV infection. Tylophorine analogs like *rac*-cryptopleurine, YXM-110, and DCB-3503 that inhibited proliferation of HepG2 cells could also be used for the treatment of HCV-associated hepatocellular carcinoma.

## 4. Experimental procedures

### 4.1. Materials and reagents

Cell culture media and fetal bovine serum (FBS) were purchased from Invitrogen (Waltham, MA, USA). All reagents were purchased from Sigma-Aldrich (St. Louis, MO, USA) except for those otherwise noted. YXM compounds were synthesized in Dr. Kuo-Hsiung Lee's laboratory, dissolved in DMSO at 500  $\mu$ M, and kept as stock solutions.<sup>12</sup>

### 4.2. Cell lines and growth conditions

HCV genotype 1b Con1 subgenomic replicon cell lines Huh-luc/neo-ET containing a luciferase reporter, and Huh 9–13 were provided by Dr. Ralf Bartenschlager from The University of Heidelberg.<sup>30,31</sup> Huh luc/neo-ET and Huh 9–13 cells were maintained in DMEM medium supplied with 10% FBS (Gibco, Waltham, MA, USA), 1 mM nonessential amino acids (Invitrogen), and 250  $\mu$ g/ml G418 (Gibco). HepG 2.2.15 cells were cultured in MEME supplemented with 10% FCS (Gibco), and 50  $\mu$ g/ml kanamycin. All cells were maintained at 37 °C in a humidified 5% CO<sub>2</sub> atmosphere.

### 4.3. Determination of anti-HCV activity by luciferase reporter assay

Firefly-luciferase reporter activity was used to monitor the replication of HCV replicons in Huh-luc/neo-ET cells free from G418.<sup>32</sup> Luciferase activity was measured with a luciferase assay kit (Promega, Madison, Wisconsin, USA) on SpectraMax M5 multi-mode microplate reader (Molecular Devices, Sunnyvale, CA, USA) according to the manufacturer's instruction.

### 4.4. Determination of HBV replication

HBV genome integrated HepG 2.2.15 cells were seeded in six-well culture plates at a density of approximately  $5 \times 10^5$  cells per well. Culture medium was changed every 2 days. Six days after seeding of cells, compounds were added to the cell cultures, and fresh medium was fed every other day for another 6 days. Cells were collected for Southern analysis for viral DNA. Total DNA was isolated by using DNeasy kits (Qiagen, Valencia, CA, USA) following the manufacturer's instructions. Twenty micrograms of DNA were separated by electrophoresis with 1% agarose and transferred to Hybond-N<sup>+</sup> membrane (Amersham Biosciences, Bucks, UK) by using the capillary transfer method with  $20 \times$  SSC overnight. After UV-crossing linking, the blot was prehybridized with 1 mg/ml salmon sperm DNA diluted in QuickHyb reagent (Invitrogen) for 1 h at 65 °C. Random <sup>32</sup>P-labeled HBV full-length probe was then added to the prehybridization reagent and hybridized overnight at 65 °C. The blot was washed with  $2 \times$  SSC/0.1% SDS twice for 5 min at room temperature and  $0.2 \times$  SSC/0.1  $\times$  SDS three times for 20 min at 65 °C. The membrane was exposed to BioMax MR Film (Kodak, Rochester, NY) at –70 °C overnight or detected by using a PhosphorImager S1 (Molecular Dynamics, Sunnyvale, CA, USA).

### 4.5. ATP hydrolysis activity assay

Preparation of recombinant Hsc70 and characterization of the ATP hydrolysis activity of Hsc70 were performed as described previously.<sup>6,33</sup> Briefly, 0.25  $\mu$ M Hsc70 was incubated in the presence or absence of various 10  $\mu$ M compound, ATP, and 0.5  $\mu$ M HCV wide-type poly U/UC RNA in 50  $\mu$ l reaction buffer (25 mM MOPS, pH 7.4, 10 mM Mg(OAc)<sub>2</sub>, 30 mM KOAc, 2 mM DTT, 1 mg/ml BSA) at 37 °C for 10 min. The reaction was stopped by adding 45% trichloro-

oacetic acid to a final concentration of 15% (v/v). The aqueous phase was washed with 1,1,2-trichlorotrifluoroethane: trioctylamine (55:45, v/v) twice. The concentration of ADP in the aqueous phase was analyzed by HPLC and determined by the standard curve generated on the same column.

#### 4.6. Affinity purification

The affinity purification was performed as described previously.<sup>26</sup> Huh-luc/neo-ET cells were lysed in protein-binding buffer (PBB, 20 mM Hepes, pH 7.9, 100 mM NaCl, 0.5 mM EDTA, 0.5% Nonidet P-40, 6 mM MgCl<sub>2</sub>, 5 mM 2-mercaptoethanol, complete protease inhibitor (Roche)). Biotinylated-*rac*-cryptopleurine was bound overnight at room temperature to a 50% slurry of streptavidin resin (Invitrogen) in buffer containing 50% DMSO and 50% PBB. Beads were washed to remove unbound compound and then incubated with recombinant Hsc70 in 2.5% BSA. Bound proteins were washed, or eluted with *rac*-cryptopleurine or its analogs. Samples were separated with SDS PAGE, and examined by Western blot.

#### 4.7. Expression and purification of recombinant CHIP

cDNA of CHIP was cloned using forward primer 5'-ATGAAGGG-CAAGGAGGAGAAGGA-3' and reverse primer 5'-AGACTCTACCGACCCACCTCTGATG-3', and inserted into the NdeI and NotI restriction enzyme sites of pET21b vector with a C-terminal histag. Recombinant proteins were overproduced in *E. coli* BL21 (DE3) pLysS cells (Promega, Madison, WI) at 22 °C for 4 h, purified by Ni<sup>2+</sup>-NTA agarose (Qiagen, Valencia, CA), and dialyzed in 50 mM HEPES/KOH, pH 7.0, containing 50 mM potassium chloride, 5 mM DTT and 10% (v/v) glycerol.

#### 4.8. Luciferase refolding assay

Refolding of chemically denatured firefly luciferase by Hsc70 in the presence or absence of tylophorine analogs was measured as described previously.<sup>34</sup> Briefly, luciferase was diluted by denaturation buffer (25 mM HEPES, pH 7.4, 50 mM KCl, 5 mM MgCl<sub>2</sub>, 6 M guanidine-HCl, 5 mM DTT) to the final concentration of 5 μM. The denaturation reaction was allowed to proceed for 40 min at 25 °C, and 1 μl aliquot was removed and mixed with 125 μl of refolding buffer (25 mM HEPES, pH 7.4, 50 mM KCl, 5 mM MgCl<sub>2</sub>, 1 mM ATP) that was supplemented with 0.25 μM Hsc70 in the presence or absence of *rac*-cryptopleurine or DCB-3503 in the presence or absence of recombinant CHIP. The refolding reaction was incubated at 25 °C. Aliquots of 4 μl were removed from the folding reactions at the indicated times and luciferase activity was measured.

#### 4.9. Statistical analysis

Data were analyzed by a two-tailed student's *t*-test using Prism Graph Pad 5.0. The difference was considered to be statistically significant when *p* < .05.

#### Acknowledgement

We are indebted to Dr. Ralf Bartenschlager for the Huh-luc/neo-ET and Huh 9-13 replicon cell lines, and pFK I389 Lucubineo NS3-3' plasmid. Dr. Yung-Chi Cheng is a fellow of the National Foundation for Cancer Research. This work was supported by grants CA177584 from National Institute of Health to KHL, PO1 CA154295 from National Cancer Institute, 5R01 AI 038204 from National Institute of Health, and a gift from William H Prusoff Foundation to YCC, Macao Science and Technology Development Fund 041/2014/A1,

Research Fund of the University of Macao MYRG2016-00105-ICMS-QRCM and MYRG2017-00116-ICMS-QRCM to YW. The funders had no role in study design, data collection and analysis, decision to publish, or preparation of the manuscript.

#### Author contributions

Y.W. designed and conducted the biology experiments. X.Y. and K.H.L. designed and synthesized tylophorine analogs. Y.C.C. designed and supervised the experiments. Y.W., S.R.C., X.Y., Y.C.C., and K.H.L. conceived, analyzed data, and wrote the manuscripts. All authors have read and approved the final manuscript.

#### Declaration of interest

The authors declare there is no conflict of interest.

#### References

1. Jarret A, McFarland AP, Horner SM, et al. Hepatitis-C-virus-induced microRNAs dampen interferon-mediated antiviral signaling. *Nat Med*. 2016;1475–1481.
2. Schinazi R, Halfon P, Marcellin P, Asselah T. HCV direct-acting antiviral agents: the best interferon-free combinations. *Liver Int*. 2014;34(Suppl. 1):69–78.
3. Tsai PC, Huang CF, Yu ML. Unexpected early tumor recurrence in patients with hepatitis C virus -related hepatocellular carcinoma undergoing interferon-free therapy: issue of tie interval between HCC treatment and antiviral therapy. *J Hepatol*. 2017;66:464.
4. Bukh J. The history of hepatitis C virus (HCV): basic research reveals unique features in phylogeny, evolution and the viral life cycle with new perspectives for epidemic control. *J Hepatol*. 2016;65(Suppl. 1):S2–S21.
5. Ahmed-Belkacem A, Colliandre L, Ahnou N, et al. Fragment-based discovery of a new family of non-peptidic small-molecule cyclophilin inhibitors with potent antiviral activities. *Nat Commun*. 2016;7:12777.
6. Wang Y, Lee S, Ha Y, et al. Tylophorine analogs allosterically regulates heat shock cognate protein 70 And inhibits hepatitis C virus replication. *Sci Rep*. 2017;7:10037.
7. Yang X, Shi Q, Lai CY, et al. Antitumor agents 295. E-ring hydroxylated antofine and cryptopleurine analogues as antiproliferative agents: design, synthesis, and mechanistic studies. *J Med Chem*. 2012;55:6751–6761.
8. Lai CY, Pan SL, Yang XM, et al. Depletion of 4E-BP1 and regulation of autophagy lead to YXM110-induced anticancer effects. *Carcinogenesis*. 2013;34:2050–2060.
9. You X, Pan M, Gao W, et al. Effects of a novel tylophorine analog on collagen-induced arthritis through inhibition of the innate immune response. *Arthritis Rheum*. 2006;54:877–886.
10. Yang X, Shi Q, Yang SC, et al. Antitumor agents 288: design, synthesis, SAR, and biological studies of novel heteroatom-incorporated antofine and cryptopleurine analogues as potent and selective antitumor agents. *J Med Chem*. 2011;54:5097–5107.
11. Semwal DK, Badoni R, Semwal R, Kothiyal SK, Singh GJ, Rawat U. The genus *Stephania* (Menispermaceae): chemical and pharmacological perspectives. *J Ethnopharmacol*. 2010;132:369–383.
12. Wang Y, Wong HC, Gullen EA, et al. Cryptopleurine analogs with modification of e ring exhibit different mechanism to *rac*-cryptopleurine and tylophorine. *PLoS One*. 2012;7:e51138.
13. Yang X, Shi Q, Lai CY, et al. Antitumor Agents 295. E-ring hydroxylated antofine and cryptopleurine analogues as antiproliferative agents: design, synthesis, and mechanistic studies. *J Med Chem*. 2012;55:6751–6761.
14. Parent R, Qu X, Petit MA, Beretta L. The heat shock cognate protein 70 is associated with hepatitis C virus particles and modulates virus infectivity. *Hepatology*. 2009;49:1798–1809.
15. Wang YP, Liu F, He HW, et al. Heat stress cognate 70 host protein as a potential drug target against drug resistance in hepatitis B virus. *Antimicrob Agents Chemother*. 2010;54:2070–2077.
16. Zhou YB, Wang YF, Zhang Y, et al. In vitro activity of cepharanthine hydrochloride against clinical wild-type and lamivudine-resistant hepatitis B virus isolates. *Eur J Pharmacol*. 2012;683:10–15.
17. Bian Z, Xiao A, Cao M, et al. Anti-HBV efficacy of combined siRNAs targeting viral gene and heat shock cognate 70. *Virology*. 2012;9:275.
18. Gao LM, Han YX, Wang YP, et al. Design and synthesis of oxymatrine analogues overcoming drug resistance in hepatitis B virus through targeting host heat stress cognate 70. *J Med Chem*. 2011;54:869–876.
19. Du NN, Li X, Wang YP, et al. Synthesis, structure-activity relationship and biological evaluation of novel N-substituted matrixin acid derivatives as host heat-stress cognate 70 (Hsc70) down-regulators. *Bioorg Med Chem Lett*. 2011;21:4732–4735.
20. Ying C, Li Y, Leung CH, Robek MD, Cheng YC. Unique antiviral mechanism discovered in anti-hepatitis B virus research with a natural product analogue. *Proc Natl Acad Sci USA*. 2007;104:8526–8531.

21. Liu C, Perilla JR, Ning J, et al. Cyclophilin A stabilizes the HIV-1 capsid through a novel non-canonical binding site. *Nat Commun.* 2016;7:10714.
22. Foster TL, Gallay P, Stonehouse NJ, Harris M. Cyclophilin A interacts with domain II of hepatitis C virus NS5A and stimulates RNA binding in an isomerase-dependent manner. *J Virol.* 2011;85:7460–7464.
23. Iwasaki S, Sasaki HM, Sakaguchi Y, Suzuki T, Tadakuma H, Tomari Y. Defining fundamental steps in the assembly of the *Drosophila* RNAi enzyme complex. *Nature.* 2015;521:533–536.
24. Chou CC, Forouhar F, Yeh YH, Shr HL, Wang C, Hsiao CD. Crystal structure of the C-terminal 10-kDa subdomain of Hsc70. *J Biol Chem.* 2003;278:30311–30316.
25. Fontaine SN, Rauch JN, Nordhues BA, et al. Isoform-selective genetic inhibition of constitutive cytosolic Hsp70 activity promotes client tau degradation using an altered co-chaperone complement. *J Biol Chem.* 2015;290:13115–13127.
26. Wang Y, Lam W, Chen SR, et al. Tylophorine analog DCB-3503 inhibited cyclin D1 translation through allosteric regulation of heat shock cognate protein 70. *Sci Rep.* 2016;6:32832.
27. Nillegoda NB, Kirstein J, Szlachcic A, et al. Crucial HSP70 co-chaperone complex unlocks metazoan protein disaggregation. *Nature.* 2015;524:247–251.
28. Lohmus A, Hafren A, Makinen K. Coat protein regulation by CK2, CPIP, HSP70, and CHIP is required for potato virus replication and coat protein accumulation. *J Virol.* 2017;91:e01316–01316.
29. Katoh H, Kubota T, Nakatsu Y, Tahara M, Kidokoro M, Takeda M. Heat shock protein 90 ensures efficient mumps virus replication by assisting with viral polymerase complex formation. *J Virol.* 2017;91:e02220–02216.
30. Vrolijk JM, Kaul A, Hansen BE, et al. A replicon-based bioassay for the measurement of interferons in patients with chronic hepatitis C. *J Virol Methods.* 2003;110:201–209.
31. Lohmann V, Korner F, Koch J, Herian U, Theilmann L, Bartenschlager R. Replication of subgenomic hepatitis C virus RNAs in a hepatoma cell line. *Science.* 1999;285:110–113.
32. Cheng Y, Tsou LK, Cai J, et al. A novel class of meso-tetrakis-porphyrin derivatives exhibits potent activities against hepatitis C virus genotype 1b replicons in vitro. *Antimicrob Agents Chemother.* 2010;54:197–206.
33. Yamagishi N, Ishihara K, Hatayama T. Hsp105alpha suppresses Hsc70 chaperone activity by inhibiting Hsc70 ATPase activity. *J Biol Chem.* 2004;279:41727–41733.
34. Lu Z, Cyr DM. Protein folding activity of Hsp70 is modified differentially by the hsp40 co-chaperones Sis1 and Ydj1. *J Biol Chem.* 1998;273:27824–27830.